

Porphyrin nanoparticles as supramolecular systems†

Charles Michael Drain,^{*ab} Gabriela Smeureanu,^a Sandeep Patel,^a
Xianchang Gong,^{*c} Jayne Garno^d and Julius Arijeloye^a

Received (in St. Louis, MO, USA) 23rd May 2006, Accepted 31st August 2006

First published as an Advance Article on the web 5th October 2006

DOI: 10.1039/b607289e

Certain applications of supramolecular porphyrinic systems, such as molecular sieves and photonics, rely on precise nanoarchitectural control of the molecules and/or atoms; therefore they require self-assembled systems of discrete arrays and highly ordered crystals. Other applications, such as oxidation catalysts for simple substrates, may be affected by the use of self-organized materials with less supramolecular order. Colloidal porphyrin nanoparticles can be considered self-organized systems that are governed by the principles of supramolecular chemistry. The formation and potential applications of nanoparticles of these chromophores are discussed in this report with special emphasis on the parameters in the methods used to make these materials, and in terms of the supramolecular chemistry. These principles, concepts, and methodologies are applicable to a wide variety of organic dyes.

“Mais Dieu a choisi celui qui est le plus parfait, c’est à dire celui qui en même temps le plus simple en hypotheses, et le plus rich en phenomenes.”‡ Gottfried Leibniz.

Introduction

Porphyrins and their related macrocycles (phthalocyanines, corroles, corrolazines, and porphyrazines) are versatile organic compounds for supramolecular chemistry because of their topological diversity, minimal conformational flexibility, and well-established synthetic methods which enable the creation of a large number of derivatives with diverse functionalities.^{1–3} Porphyrinoids are also ideal organic molecules for materials—especially photonics, sensors, and molecular sieves—because they are remarkably robust under a variety of conditions yet have optical and redox properties that can be readily fine-tuned *via* the choice of metal ion coordinated to the centre of the macrocycle and by exocyclic moieties. Nature exploits these properties by using porphyrins to harvest solar energy, transfer electrons, and as redox catalysts.⁴ Because of these properties and functions, the supramolecular chemistry of porphyrins in terms of solid state structures *self-organized* by

non-specific interactions such as dispersion forces combined with specific interactions such as coordination chemistry and hydrogen bonding continues to be of intense interest even after decades of research.^{1,5} This vigorousness is largely due to a better understanding of intermolecular forces mediated by specific interactions and to developments in synthetic and separation methodologies for the preparation of target macrocycles. Porphyrins can also be designed to *self-assemble* into discrete, predefined nano-architectures or arrays by using specific intermolecular interactions.¹ Though not *a priori* required, discrete systems usually utilize all available recognition or assembly motifs. Since the initial reports of discrete porphyrin nano-assemblies by electrostatic interactions,^{6–9} hydrogen-bonding,^{10–13} and coordination chemistry,^{14,15} there have been numerous reports on the properties of self-assembled porphyrin arrays.^{1,5}

There is a distinction between self-assembly and self-organization.¹⁶ Self-assembly is intolerant of errors and results in discrete (mono-dispersed) supramolecular arrays, albeit with varying yields. For example, the absence of a porphyrin unit in a self-assembled square array is a fatal flaw because the product is not square and has significantly different dynamic, thermodynamic, and photonic properties. Self-organization, on the other hand, is more tolerant of defects and results in non-discrete systems with varying dispersity. For example, the absence of a monomer unit from a large coordination polymer slightly alters the dimensions but not the overall structure and usually not the properties. An exception to the latter is represented by the imidazolyl polymers of Kobuke *et al.*^{17–19} The supramolecular structure of any material can be delineated, as in structural biology, by four levels of hierarchical organization.¹⁶ The primary structure describes the monomeric units and the algorithms of molecular recognition—in the present case the porphyrin serves as the core platform. The

^a Department of Chemistry and Biochemistry, Hunter College of the City, University of New York, 695 Park Avenue, New York, NY 10021, USA. E-mail: cdrain@hunter.cuny.edu; Fax: +1 212-772-5332; Tel: +1 212-650-3791

^b The Rockefeller University, 1230 York Avenue, New York, NY 10021, USA

^c Kava Technology Inc., 9505 Genesee Avenue, Suite 524, San Diego, CA 92121, USA. E-mail: xianchang@kavatechnology.com; Fax: +1 858-452-9938; Tel: +1 858-220-4707

^d Department of Chemistry, Louisiana State University, Baton Rouge, LA 70803, USA

† Electronic supplementary information (ESI) available: Nanoparticle preparations, optical spectra, analysis by DLS and AFM. See DOI: 10.1039/b607289e

‡ God has chosen that which is the most simple in hypotheses and the most rich in phenomena. “[Leibniz] essentially states that a theory has to be simpler than the data it explains, otherwise it does not explain anything”. G. Chaitin, *Scientific American*, 2006, **294**(3), 74–81. The Limits of Reason.

supramolecular architectures formed by self-assembly/organization are the secondary structures. Tertiary structures result from the self-organization of the supramolecular entities into solid-state materials, thin films, and colloids. The quaternary structure includes the interactions between the supramolecular materials and their environment, *e.g.* surfaces/matrices of the supports, thus includes interconnections with the macroscopic world.

Of course there is overlap between the various levels of organization and structure, but these concepts aid in the design of functional supramolecular materials. Self-organized systems can be used to construct colloids and to achieve maximal surface area or deployment of chromophores, such as for use as catalysts and functional coatings on surfaces.

Discrete supramolecular systems are almost always less than about 10 nm. Crystals and most solid-state structures of both discrete and polymeric supramolecular systems have dimensions from microns to many millimetres. Thus there is a void between the 3–10 nm arrays and the micron to millimetre crystals and polymers that may be filled by melding the concepts and methods of supramolecular chemistry, colloid chemistry, and surface chemistry.⁵ Part of our hypothesis is that supramolecular systems of porphyrins and related macrocycles with 5–500 nm dimensions will yield materials that will exhibit catalytic, photonic, and sensor properties that are unobtainable by either the molecular compounds or the macroscopic solids. At present the general goal is to understand and define the principles and conditions that may lead to the construction of supramolecular nanostructures of high structural integrity and provide effective algorithms for the design—by self-organization—of supramolecular materials of this intermediate, 5–500 nm scale.⁵

Supramolecular materials

It has been known for many decades that porphyrinic systems aggregate *via* π -stacking, dispersion, multipolar, and other electrostatic interactions. It is well established that the polymorphism observed in *self-assembled* crystals of a given porphyrinic system arise from different conditions used to grow the crystals.^{20–22} Analogously, it is becoming increasingly apparent that the structural landscape for *self-organized* materials of a given porphyrinoid or set of porphyrinoids is quite complex with multiple valleys (*e.g.* the numerous structures arising from the anionic tetra(4-sulfanattophenyl)porphyrin, cationic tetra(4-*N*-methylpyridinium)porphyrin, and mixtures of these).⁵ For a given macrocycle, these ordered but non-crystalline supramolecular “polymorphs” must arise from the molecular structure, preparative methods, and as importantly, environmental conditions.^{2,5,23,24} This indicates that hills rather than mountains separate the valleys in the energetics of the structural landscape.

In general there are several approaches to the formation of nanoscaled structures by non-covalent bonds. The size, polydispersity, and stability of supramolecular porphyrin polymers and aggregates are dictated by the thermodynamics of the intermolecular forces and the equilibria dictated by both energetics and environmental conditions. (1) Polymers formed *via* specific intermolecular interactions are one avenue toward

nanoscaled supramolecular materials. Single, isolated linear polymers held together only by hydrogen bonding, for example, are limited to a few monomers,^{12,13} but when coordination chemistry is used, these polymers can be significantly longer.^{25–27} Combinations of hydrogen bonding and coordinative algorithms can further enhance both structural organization and polymer size.²⁸ Thus, cooperative intermolecular interactions, *e.g.* specific intermolecular recognition motifs and non-specific interactions such as π -stacking, can result in robust self-organized systems. Self-organized systems can be highly crystalline materials or large aggregates. The specific algorithms contained in the monomers dictate the local structure, while non-specific interactions dictate the hierarchical organization of the material.^{29–32} The diverse topologies available to the porphyrins allow the design of a large number of aggregated systems.⁵ (2) Nanoscaled aggregates can also be formed using only non-specific intermolecular interactions, but with significant reduction in the hierarchical structure of the material.

For the formation of 5–500 nm materials from supramolecular polymers and other aggregates of porphyrins, the key issue is how to stabilize and isolate systems of the desired dimensions with acceptable polydispersity and in high yields.⁵ There are three basic strategies for the stabilization of nanoscaled supramolecular materials. (1) The use of stabilizing agents that are either grafted onto the porphyrin monomers or added into the solution can prevent agglomeration of the nanoparticles and result in stable colloidal dispersions.³³ (2) Kinetically trapping self-organizing materials can remove them from the conditions that allow equilibrium—usually by removing the solvent. Practically this often means isolating the nanoparticles on a surface and/while removing them from solution.^{15,16,33–41} (3) Adjusting the environmental conditions to favor or force the formation of nano aggregates by, for example, encapsulation into a solid⁴² or a gel matrix.^{43–46} Each of these strategies has advantages and disadvantages, depending on the intended function and application of the material.

Applications of porphyrin nanoparticles

The advantages of self-organizing particles over self-assembled entities arise from the use of commercially available dyes and pigments, ease of preparation, and material stability.³³ There are a variety of possible applications of nanoparticles of organic chromophores that derive from the photonic properties of both the component molecule and the nanoscaled dimensions of the particle.^{2,3,5,41,47} Many of these nanoparticles, when the porphyrin contains a redox-active transition metal (*e.g.* Fe, Co, Mn), are more efficient catalysts on a per porphyrin basis than the individual porphyrins in solution or individual porphyrins adsorbed onto supports.³³ An understanding of nanoparticle–surface interactions can be exploited to dictate the size of the deposited nanoparticles.^{34,35,37} For example, 50 nm diameter nanoparticles of hydrophilic porphyrins can be deposited onto glass surfaces passivated with a monolayer of organic ‘grease’ without further aggregation or falling apart; conversely, these nanoparticles de-aggregate into 5–20 nm particles and 5 nm high disks on hydrophilic glass surfaces. The fluorescence properties of nanoparticles

containing the free base or closed-shell metalloporphyrins, or the phosphorescence of these or other metallo derivatives such as the Pd(II) and Pt(II) can be exploited for sensors and displays.^{48–50} Since our initial report on the formation of nanoparticles of hydrophilic and hydrophobic porphyrins,³³ there has been a large body of work on the formulation of drug nanoparticles. The advantages of <60 nm diameter aggregates of drugs are manifold, including the reduction or elimination of polymorphic solid state structures, increased rate of bio-availability, and possible functionalization of the stabilizer for targeted cell delivery.⁵¹

Experimental

DLS data was collected in batch mode by a Precision Detectors Cool Batch in 0.2 mL cuvettes. The error bars represent both the average particle sizes and the entire observed distribution of particle sizes (~three standard deviations for Gaussian distributions) over the course of several different preparations by different co-workers. The error bars for just the centre of the distribution are much smaller. AFM sample preparation: glass slides (Corning) were soaked in piranha solution for 30 min, then rinsed thoroughly with deionized water. After the glass slides were dried at room temperature, 10 μ L of diluted porphyrin nanoparticle solution was transferred to the slide using a pipette. Before AFM imaging, the samples were dried for at least 4 h, then imaged in air under ambient conditions.

Porphyrin nanoparticles

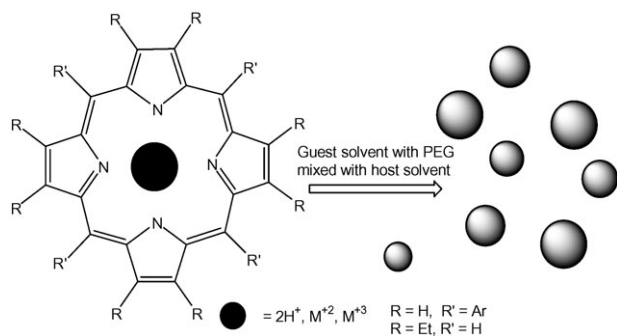
The formation of nanoscaled colloidal particles of hydrophobic porphyrins such as 5,10,15,20-tetraphenylporphyrin (TPP), 2,3,7,8,12,13,17,18-octaethylporphyrin (OEP), and many of the metallo derivatives can be accomplished by adding water (guest solvent) to a solution of a hydrophobic porphyrin in THF, DMSO, DMF, or CH₃CN (host solvent) with a few percent of a low molecular weight PEG such as HO(C₂H₄O)₄CH₃³³ or a non-ionic surfactant (Scheme 1). See supporting information for the preparation and characterization of 13 different porphyrins and metalloporphyrins.† Stabilizers such as PEG are essential for the formation of stable colloidal systems by host–guest solvent methods; reports on nanoparticle systems of porphyrinoids without this component are misleading or inaccurate since the porphyrins rapidly and quantitatively precipitate.⁵² Other inquiries into the for-

mation and activity of nanoparticles of dyes such as phthalocyanines have been reported.^{53–55} The mixed solvent approach is an efficient means to make large quantities of nanoparticle colloids (5 nm–150 nm) of a variety of porphyrins. In terms of scale-up, the particle size and distribution of batches using 20 g of porphyrin correlate well with the small batches of 20 mg.

Herein we present a variety of experiments designed to examine the molecular properties and processing variables that determine particle size and stability. The objective is three-fold: (1) to present methods to prepare porphyrinoid nanoparticles with predictable sizes; (2) to probe the intermolecular interactions that are important for nanoparticle formation; and (3) draw inferences on the hierarchical organization of the porphyrins in the nanoparticle. Porphyrin concentration, solvent, solvent ratios, amount of stabilizer, mixing speed, and temperature are significant processing variables that dictate the size and stability of the nanoparticles. The complex interplay amongst the various intermolecular interactions between solute, solvent, and stabilizer are difficult to predict *de novo*. We find that the hierarchical organization of the nanoparticles depends largely on the porphyrin structure, and that there are significant differences in nanoparticle size even with small differences in porphyrin structure.

Free base porphyrins generally need less stabilizer and less vigorous mixing compared to their metalloporphyrin analogues to form stable colloidal suspensions. For example, Zn(II)TPP requires about twice the PEG stabilizer as the free base TPP and sonication rather than vortex mixing. This observation can be heuristically explained by the increased intermolecular forces between the metalloporphyrins compared to the free bases. In this case, Zn(II) porphyrins generally have an increased proclivity to π -stack compared to the free base analogues. Conversely, the free base pyrrole N and N–H may participate in hydrogen bonding to the solvent, and in the case of nanoparticles, to the stabilizer. Macrocyclic symmetries, dipoles, and exocyclic moieties are important as well. The perfluorophenyl groups of 5,10,15,20-tetrakis(2,3,4,5,6-pentafluorophenyl)porphyrin, (TPPF₂₀) are widely recognized to impart stability to redox catalysts of the metallo derivatives,^{56–58} and to enhance the luminescence properties of especially the Pd(II) and Pt(II) species in applications such as organic LEDs and oxygen sensors.^{48–50} Since TPPF₂₀ is of wide interest we focus on some of the variables that affect colloid size and stability of this compound. These “calibration curves” illustrate general trends, but are different for each porphyrin. TPPF₂₀ forms stable nanoparticles under a wide variety of conditions: stabilizer type and concentration, host solvents, and solvent : water ratios. One reason for the wide range of processing conditions that yield stable colloids of TPPF₂₀ may be attributed to the unique solvation properties of the perfluoro-phenyl moieties. The effect of various groups on TPP derivatives on particle size and stability is also discussed for comparison.

Changes in the peripheral substituents on the porphyrin can have dramatic effects on the resultant nanoparticle size even when using identical preparative methods. Nanoparticles of 13 different porphyrins bearing a wide range of functional groups have been prepared by mixing solvents techniques.^{33†} Batch-to-batch consistency for a given porphyrin is



Scheme 1

demonstrated by dynamic light scattering (DLS) data which shows that each macrocycle results in a specific particle size with a specific dispersity for a given method. Small changes in the structure of the substituents on the macrocycle can have profound consequences in particle size, *e.g.* for TPP derivatives, when the 4-phenyl position bears an H ~ 22 nm diameter particles are formed, when it bears a methyl group 120 nm particles result, but the presence of methoxy group at the same position affords ~ 70 nm diameter particles. The metal ion within the macrocycle plays a role in determining particle size. [Fe(III)TPP]Cl[−], Co(II)TPP, and [Mn(III)TPP]Cl[−], yield 80 nm, 56 nm and 98 nm diameter particles, respectively. Thus the metal oxidation state and the presence of counter ions are also important. It is likely that similar preparative methods will result in formation of nanoparticles of many other porphyrins, metalloporphyrins and other dyes, but that the size, stability, and physical chemical properties will vary with each.^{53,54}

In addition to molecular structure, different preparative procedures also dictate particle size and stability.³³ The choice of miscible solvent, the ratio of host to guest solvent, and the rate of mixing of the two solutions, also can dictate particle size. It should be noted that not all variations in the procedures result in stable dispersions for a given porphyrin. An important consideration pertaining to metalloporphyrins is the nature of the counter ion when the oxidation state of the central metal is greater than two.

Characterization

Structure. The detailed structure inside these nanoparticles remains unknown. Densely packed, a 100 nm diameter particle of TPP (1.75 nm \times 1.75 nm \times 1 nm ~ 3 nm³) can contain up to ~ 164 000 porphyrins, but density studies and the catalytic activities of the iron porphyrins indicate that there are far fewer molecules in the aggregate. Our working hypothesis is that the nanoparticles consist of sub-domains of the macrocycles and solvent/stabilizer-filled voids or channels of unknown size and distribution, so that the number of chromophores per nanoparticle is substantially less. The structural organization of the porphyrins within the nanoparticles likely depends on the specific structure of the macrocycle used because this dictates the intermolecular interactions between the porphyrins, the solvent, and the stabilizer. Results from assays designed to probe the functional size of the domains in colloidal nanoparticles of 5,10,15,20-tetratolylporphyrin (TTP), in terms of energy/electron transfer, indicate that domains of 15–25 porphyrins act cooperatively to harvest light energy and effect electron transfer to a Fe(III)TPP acceptor. Two well-established methods were used: (i) varying the mole ratios of an acceptor dopant, and (ii) examining the optical cross section by varying the light intensity.⁵⁹ The caveat is that the antenna domain size may or may not correlate well with the physical domain size. The presence of subdomains is also consistent with AFM studies that reveal that some porphyrin nanoparticles fall apart into smaller 5–10 nm high particles on surfaces and the observation that 5–10 nm diameter nanoparticles can be prepared by sonicating the solutions as they are mixed.[†] These smaller particles can contain up to 20 and 160 porphyrins, respectively and surface

deposition studies indicate they are more robust than the much larger colloidal particles.

Optical properties. The UV-vis spectra of porphyrin nanoparticles are significantly different compared to the spectra of the corresponding porphyrin solutions. Soret bands are found to be broadened and/or split. The arrangement of macrocycles in aggregates generally fall into two types, “J” (edge-to-edge) interactions are characterized by red shifts, and “H” (face-to-face) interactions are characterized by blue shifts.⁶⁰ The optical spectra suggest both types of interactions in the nanoparticles and are well understood to be indicative of electronic coupling of the chromophores. The extent of J *versus* H aggregation depends on the specific porphyrin used. These spectra are consistent with other nanoscaled porphyrin aggregates, *e.g.* those encapsulated in MCM-41.⁴²

The aggregation of porphyrins generally results in the quenching of the fluorescence by a variety of factors such as shading the inner chromophores from light irradiation, and energy transfer and concomitant branching pathways for deactivation.^{61–63} Preliminary results from steady-state fluorescence measurements indicate that many of the freebase nanoparticles that are < 150 nm in diameter are anomalously luminescent. Comparison of the fluorescence intensity of non-aggregated porphyrins in toluene to the same porphyrin concentration in the form of colloidal nanoparticles in water, show that the latter intensity is reduced by only 20–50%. Notably, the luminescence of 140 nm diameter particles of TPPF₂₀ in water is nearly that of the same concentration of the fully solvated TPPF₂₀. This luminescence likely arises from the small ~ 10 nm diameter domains within the particles, rather than from the entire particle. The luminescence of the ~ 10 nm sub-domains is then analogous to the bright luminescence of nanoscaled aggregates of hydrophilic porphyrins^{42,62,63} and those encapsulated in zeolite-types of materials.^{64,65} Time resolved luminescence studies of the free base and Zn(II) nanoparticles may further reveal the mechanism of luminescence, domain size, and quantum efficiency.

Nanoparticle stability and dynamics

Particle stability was assayed by both DLS and UV-vis over time on batches of nanoparticles stored as they were made in closed vials in the dark in air. As noted above, the exact procedure used to prepare the nanoparticles depends on the specific porphyrin, but conditions were found that resulted in colloids that were stable for at least a month for a range of substituted macrocycles.[†] Many preparations are stable for more than a year. The nanoparticle solutions can be diluted and somewhat concentrated, but cannot be dried as this leads to irreversible agglomeration.

An inter-nanoparticle material exchange assay was designed to examine the stability of porphyrinic nanoparticles in the presence of other porphyrinic nanoparticles. In addition to examining the dynamics of particle–particle interactions, these studies were designed to assess the feasibility of using solutions with two different porphyrinic nanoparticles. The manifold applications of solutions containing two different porphyrinic nanoparticles include: (1) two different catalytic processes may be achieved concomitantly; (2) one nanoparticle is used as a

sensor for the catalytic product(s) of another nanoparticle, (3) when the different luminescent properties (*e.g.* lifetime and/or wavelength) of two or more nanoparticles are needed. Nanoparticles of free base TTP with an average particle diameter of 120 nm were mixed with nanoparticles of Fe(III)TPP with an average particle diameter of 80 nm. Two methods to assay material exchange were used. DLS indicates no changes in the two particle sizes or dispersities over the course of two weeks. A second assay monitors the fluorescence of free base TPP nanoparticles in the presence of non-luminescent Fe(III)TPP nanoparticles. Because the free base luminescence is quenched by electron transfer from the TPP to the Fe(III)TPP, any change in fluorescence intensity of this mixture over time would indicate that porphyrins form the two types of nanoparticles had exchanged. (Nanoparticles composed of both chromophores exhibit significantly reduced luminescence, *vide supra*.) The fluorescence is observed to be constant for at least six days,[†] indicating no dynamic exchange of porphyrins between particles. This is expected because of the PEG stabilizer and the water of hydration inhibit interactions between the particles and prevent agglomeration and precipitation.

Nanoparticles of TPPF₂₀

As mentioned above, colloidal nanoparticles of TPPF₂₀ are of interest because of the diverse photonic and catalytic applications. Various factors that dictate the particle size, dispersity, and stability of a variety of porphyrin nanoparticles were examined, and the results for TPPF₂₀ are illustrative of general trends. Note that the particle size and stability depends on the structure of the porphyrin/metalloporphyrin, the exact preparative procedures, and conditions in which they are examined (*e.g.* in solution, concentration, on a surface).

Stabilizer. Different stabilizers were chosen to study the effects the molecular weight and molecular properties of this component on the particle size and stability. In general, porphyrins bearing only hydro- or fluoro-carbon groups (*e.g.* TPPF₂₀, TPP, TTP) tend to form nanoparticles with sizes

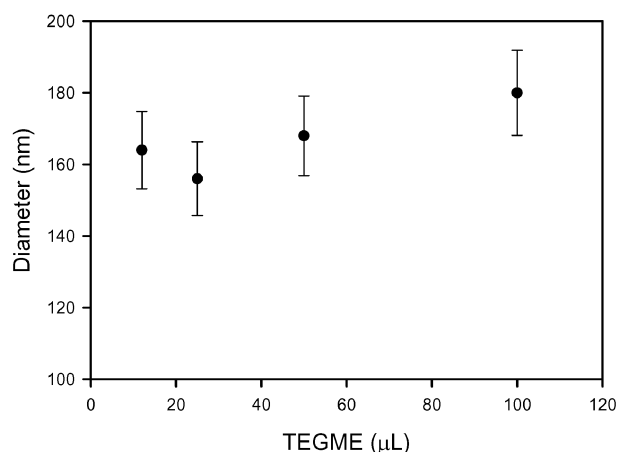


Fig. 1 DLS reveals the slight dependence of the size of TPPF₂₀ nanoparticles on TetraEGME stabilizer concentration. The indicated amount of TetraEGME was added to 0.4 mL of 39 μM TPPF₂₀ in the DMF host solvent, and 5 mL water was added *via* a pipette while mixing with a magnetic stirrer. The graph shows the average of three trials with error bars representing the distribution of particle sizes.

and distributions that are modestly dependent on the exact chemical structure and concentration of the stabilizer (Table 1, Fig. 1). Conversely, porphyrins with polar functional groups (*e.g.* *meso* pyridyl groups, and hydroxy, carboxy, amino, or sulfonato groups on the phenyl) exhibit a greater range of particle size with different kinds and amounts of the stabilizer.[†] This latter observation is likely due to the stronger interactions between the solute and the solution components (host and guest solvents, and stabilizer). Thus for polar porphyrins it is possible to tune the sizes and morphology of particles over a greater range by changing the chemical nature and the quantity of the stabilizer. The complex intermolecular interactions between amphipathic molecules such as the polyethylene glycols with water, the polar host solvent, and the porphyrin solute are essential for the formation of stable colloids.

Table 1 Stabilizer effects on nanoparticle size

Stabilizer	TPP ^a average diameter/nm	TPPF ₂₀ ^a average diameter/nm
Without stabilizer ^b	200–300	140–185
HO(CH ₂ CH ₂ O) ₃ CH ₃	25	162
HO(CH ₂ CH ₂ O) ₄ CH ₃	30	181
HO(CH ₂ CH ₂ O) ₆ H	—	182
HO(CH ₂ CH ₂ CH ₂ O) ₃ CH ₃	—	168
PEG400	Colloids not formed	152
(CH ₂ OCH ₂ CH ₂ NH ₂) ₂	232	234
	214	112
	260	98

^a Preparation method: 50 μL stabilizer was added to 0.4 mL of stock solution in DMSO (1.22 mM for TPP and 0.039 mM for TPPF₂₀), followed by adding 5 mL water with vigorous mixing. ^b There is large batch-to-batch variability and these solutions are unstable since the porphyrins precipitate after 1–2 days. HO(CH₂CH₂O)₃CH₃ = triethyleneglycolmonomethyl ether (TriEGMe); HO(CH₂CH₂O)₄CH₃ = tetraethyleneglycolmonomethyl ether (TetraEGMe); HO(CH₂CH₂O)₆H = hexaethyleneglycol (HEG); HO(CH₂CH₂CH₂O)₃CH₃ = tripropyleneglycolmonomethyl ether (TriPGMe).

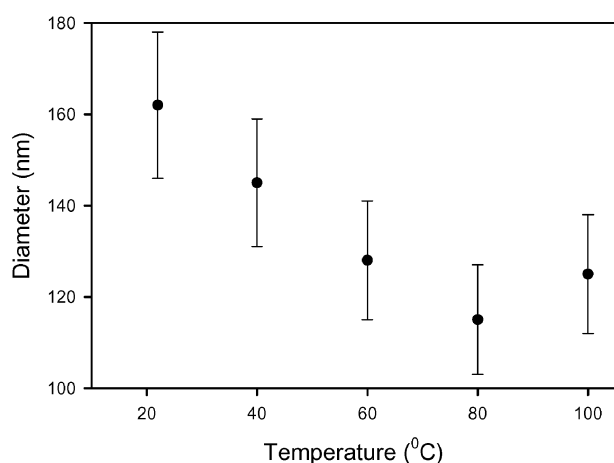


Fig. 2 The temperature during nanoparticle preparation affects the particle size. The samples were prepared at different temperatures in a water bath using 0.4 mL of a solution of 39 μM TPPF₂₀ in DMSO with 50 μL TetraEGME in a test tube followed by the addition of 5 mL water at the same temperature while mixing. The DLS measurements were taken at 25 °C upon cooling and 24 h after preparation. The graph shows the average diameters of three trials with error bars representing the entire distribution of particle sizes.

Temperature. As expected for a process dependent on intermolecular interactions, the temperature used during the preparation affects the particle size (Fig. 2) in that the particles become $\sim 25\%$ smaller as the temperature used to prepare the TPPF₂₀ sample increases from 20 °C to 100 °C. Since the particle sizes of these preparations do not change for many weeks, the stabilizer must be preventing material exchange between nanoparticles and thus preventing re-equilibration towards the larger sized nanoparticles found at room temperature. Since increasing temperatures overcome the strength of the intermolecular interactions as well as the interactions between sub-domains, smaller particle sizes are expected. The effect of temperature appears to saturate for this preparative method. The temperature at which the nanoparticles begin to form and/or the particle size at elevated temperatures are not known at this time. This kinetic trapping of nanoparticles is akin to what is observed for stacks of porphyrin nonamers.^{15,34,35,66}

Concentration. The widest range of particle sizes, about a factor of three for TPPF₂₀, can be achieved by varying the concentration of the macrocycle in the host solvent (Fig. 3). The formation of the porphyrin nanoparticles likely represents a process governed by kinetics as well as the equilibrium of intermolecular interactions between all the components. The importance of kinetics is supported by the strong dependence of particle size on concentration in the host solvent. The nonlinearity in the plot of the data suggests that the formation of these nanoparticles is a complex process; note that the largest particles form at the lowest concentrations. At the highest porphyrin concentration in the host solvent, there are some differences in the intermolecular interactions of the chromophores since a $\sim 15\%$ broadening of the Soret band is observed compared to the lowest concentration. The ob-

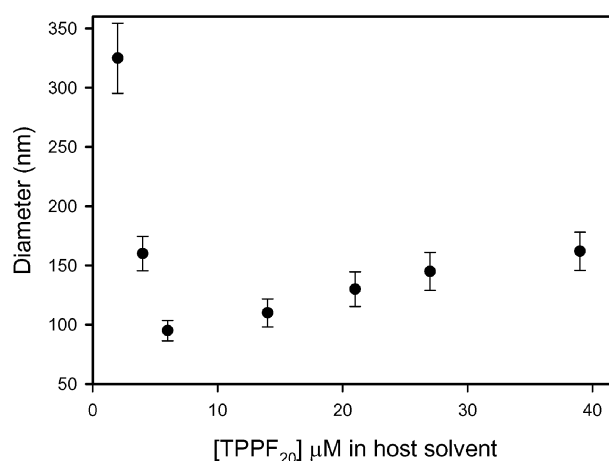


Fig. 3 The concentration of TPPF₂₀ in the DMSO host solvent strongly affects nanoparticle size as measured by DLS. A volume of 5 mL water was added to a 0.4 mL solution containing 50 μL TetraEGME and the indicated amount of the porphyrin. The graph shows the average diameters of three trials with error bars representing the entire distribution of particle sizes.

served larger nanoparticles at lower concentrations may indicate that there is a minimum, critical aggregate size that nucleates the growth, and smaller particles eventually aggregate into larger ones.

Host : guest solvent ratio and intermolecular forces. For the same considerations outlined above regarding the intermolecular forces between the components in the milieu, the chemical properties of the host solvent can have profound effects on the size and stability of the porphyrin nanoparticles (Table 2). The favourable entropy of mixing the host solvent with the guest solvent and stabilizer, as well as any enthalpic contributions such as those arising from the formation of hydrogen bonds between host and guest solvents and between the guest solvent and solute, is countered by the strength of the interactions between the dye and the host solvent. Both dipolar interactions and hydrogen bonding between the various solvents (including the stabilizer) and TPPF₂₀ are present. In addition to dipolar and H-bonding interactions, aromatic host solvents such as pyridine also afford π - π interactions with the macrocycle and the peripheral phenyl moieties.

Table 2 Effects of host solvent on the size of TPPF₂₀ nanoparticles^a

Host solvent	Nanoparticle size by DLS (average diameter, nm)
DMSO	162
DMF	166
Dimethylacetamide	400
THF	150
Pyridine	288

^a Preparation method: 50 μL TetraEGMe stabilizer was added to 0.4 mL of 0.039 mM stock solution in the host solvent, followed by adding 5 mL water with vigorous mixing. DMSO = dimethylsulfoxide, DMF = dimethylformamide, THF = tetrahydrofuran.

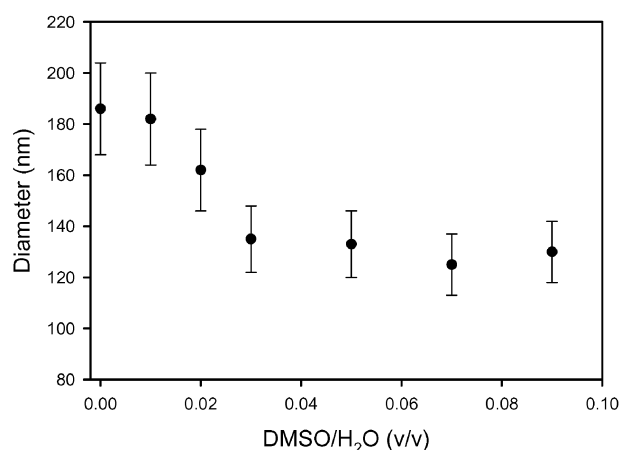


Fig. 4 The volume ratio of host solvent to guest solvent, DMSO to water in this case, affects TPPF₂₀ nanoparticle size as measured by DLS. The total porphyrin concentration was held constant at 39 μM in the mixture, as was the TetraEGME. The graph shows the average of three trials with error bars representing the entire distribution of particle sizes.

The solubility of the dye in the host solvent, the guest solvent, and the stabilizer affect the particle size and dispersity. These observations in Table 2 may somewhat correlate with the solubility of the porphyrin in the host solvent, but the concentration in a saturated solution in these solvents is within a factor of two. Also, there is no apparent correlation with dipole, dielectric, or viscosity. The observed trend, that the greater relative quantity of the host solvent to the guest solvent the smaller the particle size (Fig. 4), is consistent with other nanoparticle preparations³³ and the diminished intermolecular interactions between solute molecules.

Kinetics must also play a role here, since the diffusion/mixing the components in the mixture must be part of the agglomeration process. The greater the quantity of the host solvent results in less guest solvent to induce precipitation. Since the colloids are likely composed of sub-domains, the increased quantity of host solvent may reduce the magnitude of the inter-sub-domain interactions as well.

Mixing. The rate and efficiency of mixing the host and guest solvents have a profound effect on the size and stability of the porphyrinic nanoparticles—especially when metalloporphyrins are used. In general for a given derivative and using the same rate of addition, the greater the mixing the smaller the nanoparticles. Stirring rates were varied by controlling the spin of a magnetic stirrer, a vortex mixer was assumed to be more efficient than magnetic stirring, and sonication assumed to be the most efficient. The size of the colloidal particles of free base TPP decreases in the order: no stirring, a magnetic stir-bar with a vortex, a vortex mixer, and sonication. Conversely for TPPF₂₀ the rate of mixing has a smaller effect on particle size: stirring, vortex mixer, and sonication 140 nm, 100 nm, and 60 nm diameters. Stable metalloporphyrin particles are generally formed only when sonication is used.

Surfaces. Since many applications of organic nanoparticles will require surface deposition and it has been shown that self-

organized systems often reorganize upon interactions with surfaces,^{34,35,47} the casting of these nanoparticle solutions onto several surfaces was examined.

The aforementioned data indicate that the interactions of the porphyrins within the subdomains are stronger than the interactions between the subdomains. Therefore, it should be possible to break up the ~ 100 nm diameter colloids into the subdomains by introducing an energetic perturbation that is greater than that holding the colloid together but less than that holding the molecules in the subdomains together. *e.g.* refluxing a solution of TPPF₂₀ nanoparticles formed at room temperature (see row 3 in Table 1) for 20 minutes and allowing the solution to cool produces nanoparticles that are 20–50 nm in diameter assayed by DLS, and reassembly into the larger structures is not observed over the course of three days.

The colloidal nanoparticles also can be induced to disassemble or reorganize on surfaces that have a strong affinity for the constituent porphyrin and/or the solvents. AFM studies of nanoparticles of hydrophobic TPPF₂₀ deposited on hydrophilic glass surfaces reveal a distribution of 5–20 nm high domains that are about 50–200 nm in diameter. Conversely, AFM studies show that most of the nanoparticles of a hydrophilic porphyrin, tetra(*N*-alkylpyridinium)porphyrin⁴⁺ (water host solvent and THF guest solvent), remain intact on hydrophobic surfaces. Fig. 5 shows typical AFM on glass and mica surfaces and reveals different particle sizes on each. Table 3 summarizes AFM data shown in the supporting information on a variety of preparations deposited on hydrophilic, clean glass.

These observations also support the notion that the porphyrins in the sub-domains are held together by intermolecular interactions that are substantially greater than the forces holding the sub-domains together in the nanoparticle. For surfaces with similar hydrophobicities as the macrocycle and host solvent, as the solvent evaporates the colloids can disassemble and/or reorganize to produce smaller, 5–20 nm nanoparticles or disc-like structures that are up to several hundred nm in diameter and 2–40 nm high, *i.e.* the surface energetics dictates the degree of disaggregation or reorganization. Since the structure of the subdomains also is porphyrin

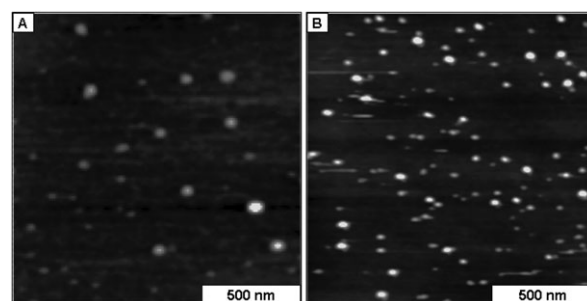



Fig. 5 AFM topographic images of TPPF₂₀ nanoparticles on ($1.5 \times 1.5 \mu\text{m}^2$); (A) mica and (B) glass. Samples were prepared by drop-deposition on freshly cleaved mica (0001) (Fig. 5A) and cleaned glass slides (Fig. 5B). 400 μL of a stock solution of 3.4 mg porphyrin in 4 mL DMSO was added to 5 mL water containing different stabilizers (5A- TriPGME and 5B- TetraEGME). Then, 20 μL of the nanoparticle suspension was deposited on 1×1 cm piece of glass or mica, dried overnight, imaged in air using tip with a 0.5 N m^{-1} spring constant.

Table 3 Average AFM heights of TPPF₂₀ colloids deposited onto hydrophilic glass surfaces

Stabilizer host solvent	Average diameter of colloids in solution by DLS	Average height of nanoparticles on glass by AFM/nm ^a
None	—	—
DMSO	185 ^b	5–40
HO(CH ₂ CH ₂ O) ₄ CH ₃ pyridine	170	9 ± 6
HO(CH ₂ CH ₂ O) ₄ CH ₃ DMSO	181	30 ± 15
HO(CH ₂ CH ₂ CH ₂ O) ₃ CH ₃ DMSO	167	6 ± 4

Preparation method: 50 µL stabilizer was added to 0.4 mL of 0.040 mM stock solution in the host solvent, followed by adding 5 mL water with vigorous mixing or sonication.^a For AFM studies, the stock solutions are diluted with water by a factor of 3–5, and drop cast onto glass slides that have been cleaned by ozone or treatment with piranha solution (3 : 1 mixture of sulfuric acid and 30% hydrogen peroxide).^b The colloidal solution is stable for less than 1–2 days.

Table 4 Catalytic epoxidation of cyclohexene of a homogeneous solution of FeTPPF₂₀ versus a solution of nanoparticles of the same porphyrin

Porphyrin	Solution	35 nm nanoparticles
		
A	68.9%	73.5%
B	68.9	73.5
C	13.2	15.7
D	17.9	10.7
E	223	16 511

Reaction conditions: Homogeneous reaction conditions were carried out in CH₃CN at room temperature for 24 h, nanoparticles were prepared using DMF as host solvent and water as guest and TEGME as stabilizer.† A catalyst : PhIO : alkene molar ratio of 1 : 2527 : 40555, was used and pinene was added as the external standard. A: yields based on iodobenzene, B: percentage of cyclohexene oxide in product, C: percentage of cyclohexen-3-one in product, D: percentage of cyclohexen-3-ol in product, E: turn over numbers. Product identification was confirmed by GC-MS.

dependent, the structure of the small surface-absorbed particles differs from porphyrin to porphyrin. These results indicate that tuning of surface energetics in terms of hydrophobicity can be used to dictate particle size or other morphology. This observation also suggests that solvent flow and evaporation dynamics may enable the patterning of these small nanoparticles.

Both AFM and DLS were used to measure the size distribution of nanoparticle preparations. When using DLS, information regarding the aggregation of nanoparticles can be gained in various solvents, while with AFM, measurements could be made in the absence of solvents. In some preparations, the histograms of each seem to evidence a bimodal distribution. In the DLS, the relatively low concentration of smaller peaks likely represents some of the subdomains that have not aggregated into the larger particles. Conversely in the AFM, the reorganizing nanoparticles may not have reached equilibrium as the solvent evaporates.

Nanoparticle catalysis

Table 4 presents data comparing the catalytic activity of Fe(III)TPPF₂₀Cl in CH₃CN versus nanoparticles of the same solution. Note that there is *ca.* 80-fold increase in the turnover numbers and a different ratio of the products arising from allylic hydrogen atom abstraction pathway (the alcohol and ketone). Given that the generally accepted mechanism for catalyst deactivation is the oxidation of the porphyrin ring, these results are counter intuitive. Our working hypothesis is

that both the metalloporphyrins on the surface of the nanoparticle and those on the surface of the subdomains are the active catalytic entities, and that the substrate diffuses into the voids between the subdomains of the larger particle. The inner macrocycles then serve as a structural support to reduce self-oxidation and destruction of the catalyst. This data shows the importance of understanding the supramolecular interactions within the nanoparticle and attests to the functional differences of the nanoparticles versus the fully solvated porphyrin. A complete investigation of the catalytic properties is ongoing.

Conclusions

Recent reports on nanoparticles of other porphyrinoids, and nanoarchitectures with different morphologies such as nanotubes, have shown that the formation of nanostructured materials by self-organization is general. The hierarchical organization is dictated by both the molecules and by the preparative methods. The nanoscale size imparts functionalities unobtainable by the molecule or macroscopic material.^{53,54,66–71} The evaluation of the physical, chemical, and functional properties of nanoparticles of other dye systems will also provide a portal to materials that exhibit enhanced or new functionalities (*e.g.* catalytic, sensing, luminescent) compared to the known properties of the component molecules, for example the free base and closed shell metalloporphyrin nanoparticles discussed above. The variety of other complex porphyrinic materials with nanostructured features,^{5,23,24} indicates the richness of the possible structures that can be

obtained using these ~ 1 nm rigid macrocycles appended with appropriate motifs for specific or non-specific supramolecular interactions. The richness of the supramolecular chemistry and the ability to kinetically trap the self-organized porphyrinic systems affords nanoscaled colloids of various sizes. Surfactants that form nanoscaled, metastable structures such as those used to form zeolites, trimethylcetylammmonium bromide and Triton X-100, may well serve to template the formation of other nanoscaled tubular or rod-like architectures of porphyrins.⁵ Since porphyrinic compounds are the basis of Photo Dynamic Therapy—which has a multi-billion dollar yearly market world wide—formulations of porphyrinic nanoparticles may significantly improve the delivery of these types of therapeutics.

Acknowledgements

This work was supported by the National Science Foundation (DMI-0232002 to Kava Technology and CHE-0554703 to CMD), The National Institutes of Health (SCORE S06GM60654 to CMD). Hunter College Chemistry infrastructure is supported by the National Science Foundation, National Institutes of Health, including the RCMI program (G12-RR-03037), and the City University of New York. J. A. thanks the MBRS for support.

References

- C. M. Drain, I. Goldberg, I. Sylvain and A. Falber, *Top. Curr. Chem.*, 2005, **245**, 55–88.
- C. M. Drain, G. Smeureanu, J. Batteas and S. Patel, in *Dekker Encyclopaedia of Nanoscience and Nanotechnology*, eds. J. A. Schwartz, C. I. Contescu and K. Putyera, Marcel Dekker Inc., New York, 2004, vol. 5, pp. 3481–3502.
- C. M. Drain and X. Chen, in *Encyclopedia of Nanoscience & Nanotechnology*, ed. H. S. Nalwa, American Scientific Press, New York, 2004, vol. 9, pp. 593–616.
- D. C. Mauzerall, *Clin. Dermat.*, 1998, **16**, 195–201.
- C. M. Drain, G. Bazzan, T. Milic, M. Vinodu and J. C. Goeltz, *Isr. J. Chem.*, 2005, **45**, 255–269.
- C. M. Drain, B. Christensen and D. C. Mauzerall, *Proc. Natl. Acad. Sci. USA*, 1989, **86**, 6959–6962.
- C. M. Drain and D. C. Mauzerall, *Bioelectrochem. Bioenerg.*, 1990, **24**, 263–266.
- C. M. Drain and D. C. Mauzerall, *Biophys. J.*, 1992, **63**, 1544–1555.
- C. M. Drain and D. C. Mauzerall, *Biophys. J.*, 1992, **63**, 1556–1563.
- C. M. Drain, R. Fischer, E. Nolen and J. M. Lehn, *J. Chem. Soc., Chem. Commun.*, 1993, 243–245.
- C. M. Drain and X. Gong, *Chem. Commun.*, 1997, 2117–2118.
- X. Shi, K. M. Barkigia, J. Fajer and C. M. Drain, *J. Org. Chem.*, 2001, **66**, 6513–6522.
- C. M. Drain, X. Shi, T. Milic and F. Nifatis, *Chem. Commun.*, 2001, 287–288 (Addendum p. 1418).
- C. M. Drain and J.-M. Lehn, *J. Chem. Soc., Chem. Commun.*, 1994, 2313–2315 (correction 1995, p. 2503).
- C. M. Drain, F. Nifatis, A. Vasenko and J. D. Batteas, *Angew. Chem., Int. Ed.*, 1998, **37**, 2344–2347.
- C. M. Drain, *Proc. Natl. Acad. Sci. USA*, 2002, **99**, 5178–5182.
- Y. Kuramochi, A. Satake and Y. Kobuke, *J. Am. Chem. Soc.*, 2004, **126**, 8668–8669.
- Y. Kobuke, *J. Porphyrins Phthalocyanines*, 2004, **8**, 156–174.
- Y. Kobuke and N. Nagata, *Mol. Cryst. Liq. Cryst.*, 2000, **342**, 51–56.
- M. P. Byrn, C. J. Curtis, I. Goldberg, Y. Hsiou, S. I. Khan, P. A. Sawin, S. K. Tendick and C. E. Strouse, *J. Am. Chem. Soc.*, 1991, **113**, 6549–6557.
- Y. Diskin-Posner, R. K. Kumar and I. Goldberg, *New J. Chem.*, 1999, **23**, 885–890.
- Y. Diskin-Posner and I. Goldberg, *Chem. Commun.*, 1999, 1961–1962.
- Z. Wang, C. J. Medforth and J. A. Shellnutt, *J. Am. Chem. Soc.*, 2004, **126**, 16720–16721.
- Z. Wang, C. J. Medforth and J. A. Shellnutt, *J. Am. Chem. Soc.*, 2004, **126**, 15954–15955.
- C.-T. Chen and K. S. Suslick, *Coord. Chem. Rev.*, 1993, **128**, 293–322.
- B. Moulton and M. J. Zaworotko, *Curr. Opin. Solid State Mater. Sci.*, 2002, **6**, 117–123.
- M. Shmilovits, M. Vinodu and I. Goldberg, *Cryst. Growth Des.*, 2004, **4**, 633–638.
- M. Shmilovits, M. Vinodu and I. Goldberg, *New J. Chem.*, 2004, **28**, 223–227.
- T. S. Balaban, A. Eichhofer and J.-M. Lehn, *Eur. J. Org. Chem.*, 2000, **24**, 4047–4057.
- T. S. Balaban, A. D. Bhise, M. Fischer, M. Linke-Schaetzel, C. Roussel and N. Vanthuyne, *Angew. Chem., Int. Ed.*, 2003, **42**, 2140–2144.
- T. S. Balaban, R. Goddard, M. Linke-Schaetzel and J. M. Lehn, *J. Am. Chem. Soc.*, 2003, **125**, 4233–4239.
- M. Linke-Schaetzel, A. D. Bhise, H. Gliemann, T. Koch, T. Schimmel and T. S. Balaban, *Thin Solid Films*, 2004, **451–52**, 16–21.
- X. Gong, T. Milic, C. Xu, J. D. Batteas and C. M. Drain, *J. Am. Chem. Soc.*, 2002, **124**, 14290–14291.
- T. N. Milic, N. Chi, D. G. Yablon, G. W. Flynn, J. D. Batteas and C. M. Drain, *Angew. Chem., Int. Ed.*, 2002, **41**, 2117–2119.
- C. M. Drain, J. D. Batteas, G. W. Flynn, T. Milic, N. Chi, D. G. Yablon and H. Sommers, *Proc. Natl. Acad. Sci., USA*, 2002, **99**, 6498–6502.
- M. C. Lensen, K. Takazawa, J. Elemans, C. Jeukens, P. C. M. Christianen, J. C. Maan, A. E. Rowan and R. J. M. Nolte, *Chem.–Eur. J.*, 2004, **10**, 831–839.
- J. Elemans, A. E. Rowan and R. J. M. Nolte, *J. Mater. Chem.*, 2003, **13**, 2661–2670.
- J. Elemans, R. J. M. Nolte and A. E. Rowan, *J. Porphyrins Phthalocyanines*, 2003, **7**, 249–254.
- L. Latterini, R. Blossey, J. Hofkens, P. Vanoppen, F. C. De Schryver, A. E. Rowan and R. J. M. Nolte, *Langmuir*, 1999, **15**, 3582–3588.
- J. Foekema, A. P. H. J. Schenning, D. M. Vriezema, F. B. G. Benneker, K. Norgaard, J. K. M. Kroon, T. Bjornholm, M. Feiters, A. E. Rowan and R. J. M. Nolte, *J. Phys. Org. Chem.*, 2001, **14**, 501–512.
- X. Chen, L. Hui, D. A. Foster and C. M. Drain, *Biochemistry*, 2004, **43**, 10918–10929.
- W. Xu, H. Guo and D. L. Akins, *J. Phys. Chem. B*, 2001, **105**, 1543–1546.
- T. Komatsu, E. Tsuchida, C. Böttcher, D. Donner, C. Messerschmidt, U. Siggel, W. Stocker, J. P. Rabe and J.-H. Fuhrhop, *J. Am. Chem. Soc.*, 1997, **119**, 11660–11665.
- M. Shirakawa, S.-i. Kawano, N. Fujita, K. Sada and S. Shinkai, *J. Org. Chem.*, 2003, **68**, 5037–5044.
- D. M. Togashi, S. M. B. Costa, A. Sobral and A. Gonsalves, *J. Phys. Chem. B*, 2004, **108**, 11344–11356.
- P. Terech, C. Scherer, B. Deme and P. Ramasseul, *Langmuir*, 2003, **19**, 10641–10647.
- T. Milic, J. C. Garno, G. Smeureanu, J. D. Batteas and C. M. Drain, *Langmuir*, 2004, **20**, 3974–3983.
- G. Khalil, M. Gouterman, S. Ching, C. Costin, L. Coyle, S. Gouin, E. Green, M. Sadilek, R. Wan, J. Yearyearn and B. Zelelow, *J. Porphyrins Phthalocyanines*, 2002, **6**, 135–145.
- B. Zelelow, G. E. Khalil, G. Phelan, B. Carlson, M. Gouterman, J. B. Callis and L. R. Dalton, *Sens. Actuators, B*, 2003, **96**, 304–314.
- G. E. Khalil, A. Chang, M. Gouterman, J. B. Callis, L. R. Dalton, N. J. Turro and S. Jockusch, *Rev. Sci. Instrum.*, 2005, **76**, 1–8.
- X. Chen and C. M. Drain, *Drug Design Rev.-Online*, 2004, **1**, 215–234, <http://www.bentham.org/ddro/>.
- Y. Takahashi, H. Kasai, H. Nakanishi and T. M. Suzuki, *Angew. Chem., Int. Ed.*, 2006, **45**, 913–916.
- (a) C. Nitschke, S. M. O'Flaherty, M. Kroll and W. J. Blau, *J. Phys. Chem. B*, 2004, **108**, 1287–1295; (b) A. de la Escosura, M. V.

- Martinez-Diaz, P. Thordarson, A. E. Rowan, R. J. M. Nolte and T. Torres, *J. Am. Chem. Soc.*, 2003, **125**, 12300–12308.
- 54 C. Nitschke, S. M. O'Flaherty, M. Kroll, J. J. Doyle and W. J. Blau, *Chem. Phys. Lett.*, 2004, **383**, 555–560.
- 55 I. Y. Denisyuk and N. V. Kamanina, *Opt. Spectrosc.*, 2004, **96**, 235–239.
- 56 M. W. Grinstaff, M. G. Hill, J. A. Labinger and H. B. Gray, *Science*, 1994, **264**, 1311–1313.
- 57 M. Selke, M. F. Sisemore and J. S. Valentine, *J. Am. Chem. Soc.*, 1996, **118**, 2008–2012.
- 58 T. Ikeue, Y. Ohgo, T. Saitoh, T. Yamaguchi and M. Nakamura, *Inorg. Chem.*, 2001, **40**, 3423–3434.
- 59 D. Mauzerall and N. L. Greenbaum, *Biochim. Biophys. Acta*, 1989, **974**, 119–140.
- 60 (a) M. Kasha, H. R. Rawls and M. A. El-Bayoum, *Pure Appl. Chem.*, 1965, **11**, 371–381; (b) C. A. Hunter and J. K. M. Sanders, *J. Am. Chem. Soc.*, 1990, **112**, 5525–5534.
- 61 S.-S. Sun and A. J. Lees, *Coord. Chem. Rev.*, 2002, **230**, 170–191.
- 62 A. V. Udaltsov, L. A. Kazarin and A. A. Sweshnikov, *J. Mol. Struct.*, 2001, **562**, 227–239.
- 63 S. Okada and H. Segawa, *J. Am. Chem. Soc.*, 2003, **125**, 2792–2796.
- 64 D. L. Akins, S. Ozcelik, H. R. Zhu and C. Guo, *J. Phys. Chem.*, 1996, **100**, 14390–14396.
- 65 D. L. Akins, H. R. Zhu and C. Guo, *J. Phys. Chem.*, 1996, **100**, 5420–5425.
- 66 C. M. Drain, J. T. Hupp, K. S. Suslick, M. R. Wasielewski and X. Chen, *J. Porphyrins Phthalocyanines*, 2002, **6**, 241–256.
- 67 T. Hasobe, H. Imahori, S. Fukuzumi and P. V. Kamat, *J. Mater. Chem.*, 2003, **13**, 2515–2520.
- 68 Y. N. Konan, R. Cerny, J. Favet, M. Berton, R. Gurny and E. Allemann, *Eur. J. Pharm. Biopharm.*, 2003, **55**, 115–124.
- 69 T. van der Boom, R. T. Hayes, Y. Zhao, P. J. Bushard, E. A. Weiss and M. R. Wasielewski, *J. Am. Chem. Soc.*, 2002, **124**, 9582–9590.
- 70 M. K. Nazeeruddin, R. Hunphry-Baker, D. L. Officer, W. M. Campbell, A. K. Burrell and M. Graetzel, *Langmuir*, 2004, **20**, 6514–6517.
- 71 M. J. Ahrens, L. E. Sinks, B. Rybtchinski, W. H. Liu, B. A. Jones, J. M. Giaimo, A. V. Gusev, A. J. Goshe, D. M. Tiede and M. R. Wasielewski, *J. Am. Chem. Soc.*, 2004, **126**, 8284–8294.